# Emission and Metal- and Ligand-Centered-Redox Characteristics of the Hexarhenium(III) Clusters *trans*- and *cis*-$[Re_6(\mu_3\text{-}S)_8Cl_4(L)_2]^{2-}$, Where L Is a Pyridine Derivative or Pyrazine

**Takashi Yoshimura, Keisuke Umakoshi,† Yoichi Sasaki,* Shoji Ishizaka, Haeng-Boo Kim, and Noboru Kitamura**

Division of Chemistry, Graduate School of Science, Hokkaido University, Sapporo, 060-0810, Japan

*Received November 5, 1999*

Preparations of a series of face-capped octahedral hexarhenium(III) clusters having two N-heterocyclic ligands, $[Bu_4N]_2[trans\text{-}\{Re_6(\mu_3\text{-}S)_8Cl_4(L)_2\}]$ ($Bu_4N^+$ = tetra-*n*-butylammonium cation; L = pyrazine (**1a**), 4,4′-bipyridine (**3a**), 4-methylpyridine (**5a**), 4-(dimethylamino)pyridine (**6a**)) and their cis analogues (**1b**, **3b**, **5b**, and **6b**, respectively), and their electrochemical and photophysical properties have been reported. An X-ray crystal structure determination has been carried out for **1a** to confirm the trans configuration ($C_{40}H_{80}N_6S_8Cl_4Re_6$, orthorhombic, space group *Cmca* (No. 64), $a = 19.560(5)$ Å, $b = 19.494(4)$ Å, $c = 18.592(4)$ Å, $\beta = 115.76(2)°$, $Z = 4$). The redox potential of the reversible $Re^{III}_6/Re^{III}_5Re^{IV}$ process of these complexes and previously reported $[Bu_4N]_2$-[*trans*- and *cis*-$\{Re_6(\mu_3\text{-}S)_8Cl_4$(4-cyanopyridine)$_2\}$] (**2a** and **2b**, respectively) and $[Bu_4N]_2[trans$- and *cis*-$\{Re_6(\mu_3\text{-}S)_8Cl_4(pyridine)_2\}]$ (**4a** and **4b**, respectively) in acetonitrile depends linearly on the p$K_a$ of the N-heterocyclic ligands, with the potentials being more negative with basic ligands. The ligand-centered-redox waves for **1a**, **1b**, **2a**, and **2b** were observed as split waves ($\Delta E_{1/2} = 90-140$ mV), the extent of the splitting being larger for the cis isomer and largest for the pyrazine complexes. Electronic interaction between the two ligands through the $[Re_6(\mu_3\text{-}S)_8]^{2+}$ core has been suggested. The second ligand-reduction wave was also observed for **3a** and **3b**, the potential being shifted positively to coalesce with the first reduction wave on addition of the weak proton donor imidazole. This is accounted for by the proton-coupled redox reaction at the free pyridyl site of the 4,4′-bipyridine ligands. All of the complexes show luminescence in acetonitrile at room temperature. While the complexes of pyridine and 4-methylpyridine show photophysical characteristics ($\lambda_{em}$ 740−750 nm, $\phi_{em}$ 0.031−0.057, $\tau_{em}$ 4.2−6.2 $\mu$s) similar to those (770 nm, 0.039, and 6.3 $\mu$s, respectively) of $[Re_6(\mu_3\text{-}S)_8Cl_6]^{4-}$, emissions of other complexes are significantly weak with $\lambda_{em}$, $\phi_{em}$, and $\tau_{em}$ values in the ranges 763−785 nm, 0.0010−0.0017, and 0.013−0.029 $\mu$s, respectively. Suggestions are given for the excited states localized on the cluster core and the ligand $\pi^*$ orbitals.

## Introduction

Hexarhenium(III) chalcogenide clusters with $[Re_6(\mu_3\text{-}E)_8]^{2+}$ cores (E = S, Se, Te) have been the subject of recent extensive studies.[1−14] Versatility of the clusters has been proved by several synthetic approaches that obtain variety of derivatives. Mixed-cap clusters composed of different chalcogenide ligands and chalcogenide−halide combinations have been prepared by controlling the amount of starting materials for the solid-state syntheses of the cluster units.[15−29] Supramolecules and

† Present address: Department of Applied Chemistry, Faculty of Engineering, Nagasaki University, Nagasaki 852-8521, Japan.

(1) Saito, T. *J. Chem. Soc., Dalton Trans.* **1999**, 97−105.
(2) Arratia-Perez, R.; Hernandez-Acevedo, L. *J. Chem. Phys.* **1999**, *110*, 2529−2532.
(3) Shores, M. P.; Beauvais, L. G.; Long, J. R. *J. Am. Chem. Soc.* **1999**, *121*, 775−779.
(4) Shores, M. P.; Beauvais, L. G.; Long, J. R. *Inorg. Chem.* **1999**, *38*, 1648−1649.
(5) Wang, R.; Zheng, Z. *J. Am. Chem. Soc.* **1999**, *121*, 3549−3550.
(6) Zheng, Z.; Gray, T. G.; Holm, R. H. *Inorg. Chem.* **1999**, *38*, 4888−4895.
(7) Arratia-Perez, R.; Hernandez-Acevedo, L. *J. Chem. Phys.* **1999**, *111*, 168−172.
(8) Yoshimura, T.; Ishizaka, S.; Umakoshi, K.; Sasaki, Y.; Kim, H.-B.; Kitamura, N. *Chem. Lett.* **1999**, 697−698.
(9) Yoshimura, T.; Ishizaka, S.; Sasaki, Y.; Kim, H.-B.; Kitamura, N.; Naumov, N. G.; Sokolov, M. N.; Fedorov, V. E. *Chem. Lett.* **1999**, 1121−1122.
(10) Yoshimura, T.; Umakoshi, K.; Sasaki, Y.; Sykes, A. G. *Inorg. Chem.* **1999**, *38*, 5557−5564.
(11) Guilbaud, C.; Deluzet, A.; Domercq, B.; Molinie, P.; Coulon, C.; Boubekeur, K.; Batail, P. *Chem. Commun.* **1999**, 1867−1868.
(12) Gray, T. G.; Rudzinski, C. M.; Nocera, D. G.; Holm, R. H. *Inorg. Chem.* **1999**, *38*, 5932−5933.
(13) Decker, A.; Simon, F.; Boubekeur, K.; Fenske, D.; Batail, P. *Z. Anorg. Allg. Chem.* **2000**, *626*, 309−313.
(14) Kobayashi, N.; Ishizaka, S.; Yoshimura, T.; Kim, H.-B.; Sasaki, Y.; Kitamura, N. *Chem. Lett.* **2000**, 134−135.
(15) Perrin, A. *New J. Chem.* **1990**, *14*, 561−567.
(16) Yaghi, O. M.; Scott, M. J.; Holm, R. H. *Inorg. Chem.* **1992**, *31*, 4778−4784.
(17) Penicaud, A.; Boubeker, K.; Batail, P.; Canadell, E.; Auban-Senzier, P.; Jerome, D. *J. Am. Chem. Soc.* **1993**, *115*, 4101−4112.
(18) Gabriel, J.-C.; Boubekeur, K.; Batail, P. *Inorg. Chem.* **1993**, *32*, 2894−2900.
(19) Uriel, S.; Boubeker, K.; Batail, P.; Orduna, J.; Canadell, E. *Inorg. Chem.* **1995**, *34*, 5307−5313.
(20) Dolbecq, A.; Boubekeur, K.; Batail, P.; Canadell, E.; Auban-Senzier, P.; Coulon, C.; Lerstrup, K.; Bechgaard, K. *J. Mater. Chem.* **1995**, *5*, 1707−1718.
(21) Mironov, Y. V.; Virovets, A. V.; Fedorov, V. E.; Podberezskaya, N. V.; Shishkin, O. V.; Struchkov, Y. T. *Polyhedron* **1995**, *14*, 3171−3173.
(22) Dolbecq, A.; Fourmigue, M.; Batail, P. *Bull. Soc. Chim. Fr.* **1996**, *133*, 83−88.
(23) Uriel, S.; Boubekeur, K.; Batail, P.; Orduna, J. *Angew. Chem., Int. Ed. Engl.* **1996**, *35*, 1544−1547.
(24) Mironov, Y. V.; Cody, J. A.; Albrecht-Schmitt, T. E.; Pell, M. A.; Ibers, J. A. *J. Am. Chem. Soc.* **1997**, *119*, 493−498.
(25) Yarovoi, S. S.; Mironov, Yu. I.; Mironov, Yu. V.; Virovets, A. V.; Fedorov, V. E. *Mater. Res. Bull.* **1997**, *32*, 1271−1277.

10.1021/ic991282a CCC: $19.00 
Published on Web 03/23/2000

crystalengineering based on the $[Re_6(\mu_3\text{-}E)_8]^{2+}$ core have been reported recently.[3,5,6,30−34] Examples are the cyano-bridged aggregated complexes having three-dimensional Re−CN−M frameworks such as $Cs_2Mn_3[Re_6(\mu_3\text{-}Se)_8(CN)_6]_2\cdot 15H_2O$, $(H_3O)_2Co_3[Re_6(\mu_3\text{-}Se)_8(CN)_6]_2\cdot 14.5H_2O$, and $M_4[Re_6(\mu_3\text{-}Se)_8(CN)_6]_3\cdot xH_2O$ (M = Ga, Fe).[3,30] In addition to their synthetic versatility, redox-active[6,35−37] and luminescent properties[2,7−9,11,12,14] reported for some $[Re_6(\mu_3\text{-}E)_8]^{2+}$ complexes demonstrate that there may be further applications for this class of cluster complexes.

The substitution of trialkylphosphine for the terminal halides in $[Re_6(\mu_3\text{-}E)_8X_6]^{4-}$ (E = S, Se; X = halide) was controlled by the amount of phosphine and the reaction temperature and duration to give a series of the substituted complexes, $[Re_6(\mu_3\text{-}E)_8X_{6-n}(PEt_3)_n]^{(4-n)-}$ (E = Se, $n$ = 3−6; E = S, $n$ = 2−6).[36,37] We recently reported the controlled synthesis of a series of pyridine (py) and 4-cyanopyridine (cpy) complexes, $[Re_6(\mu_3\text{-}S)_8Cl_{6-n}(L)_n]^{(4-n)-}$ (L = py, $n$ = 2−4; L = cpy, $n$ = 2).[10] For the complexes with $n$ = 2, both trans and cis isomers were isolated. The substitution-inert nature of the terminal sites (X) of $[Re_6(\mu_3\text{-}E)_8X_6]^{4-}$ complexes is a key to the controlled syntheses of the complexes with various combinations of terminal ligands, and because of this inertness, designed syntheses of various new derivatives of the $[Re_6(\mu_3\text{-}E)_8]^{2+}$ core are highly promising. While studying the cpy derivatives, we found that the two chemically equivalent cpy ligands coordinated in a trans or cis orientation to the $[Re_6(\mu_3\text{-}S)_8]^{2+}$ core show splitting of the ligand-reduction wave in the cyclic voltammograms. This splitting indicates that there is a redox interaction between the ligands through the hexarhenium core. We also found that these py complexes show strong luminescence at room temperature. To obtain further systematic information on the redox interaction of the ligands through the hexarhenium core as well as on the photoluminescent properties, we introduced new N-heterocyclic ligands such as pyrazine (pz), 4,4-bipyridine (bpy), 4-methylpyridine (mpy), and (4-dimethylamino)pyridine (dmap). Nine new $[Re_6(\mu_3\text{-}S)_8]^{2+}$ clusters, [*trans*- and *cis*-$\{Re_6(\mu_3\text{-}S)_8Cl_4(L)_2\}]^{2-}$ and [*mer*-$\{Re_6(\mu_3\text{-}S)_8Cl_3(bpy)_3\}]^{-}$, summarized in Chart 1, are reported in this paper. The pz, bpy, and cpy ligands are able to be reduced, so that the ligand−ligand interactions in their $Re_6$ complexes are discussed on the basis of the extent of splitting of the ligand-based redox processes in the cyclic and differential-pulse voltammograms. Proton-coupled electron transfer properties of the bpy complexes are investigated and photoluminescent properties of the new complexes and those of the previously reported py complexes[10] are also discussed.

**Chart 1**

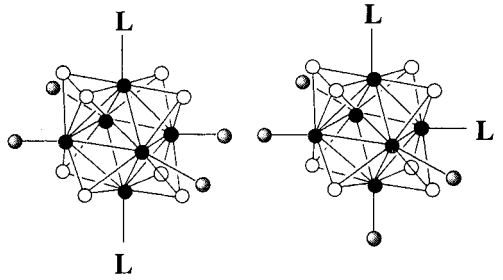


trans-isomer cis-isomer

| L | pKa | |
|---|---|---|
| pz | 0.65 | *trans*-$[Re_6(\mu_3\text{-}S)_8Cl_4(pz)_2]^{2-}$ (**1a**) |
| | | *cis*-$[Re_6(\mu_3\text{-}S)_8Cl_4(pz)_2]^{2-}$ (**1b**) |
| cpy | 1.9 | *trans*-$[Re_6(\mu_3\text{-}S)_8Cl_4(cpy)_2]^{2-}$ (**2a**) |
| | | *cis*-$[Re_6(\mu_3\text{-}S)_8Cl_4(cpy)_2]^{2-}$ (**2b**) |
| bpy | 4.44 | *trans*-$[Re_6(\mu_3\text{-}S)_8Cl_4(bpy)_2]^{2-}$ (**3a**) |
| | | *cis*-$[Re_6(\mu_3\text{-}S)_8Cl_4(bpy)_2]^{2-}$ (**3b**) |
| | | *mer*-$[Re_6(\mu_3\text{-}S)_8Cl_3(bpy)_3]^{-}$ (**3c**) |
| py | 5.25 | *trans*-$[Re_6(\mu_3\text{-}S)_8Cl_4(py)_2]^{2-}$ (**4a**) |
| | | *cis*-$[Re_6(\mu_3\text{-}S)_8Cl_4(py)_2]^{2-}$ (**4b**) |
| mpy | 6.02 | *trans*-$[Re_6(\mu_3\text{-}S)_8Cl_4(mpy)_2]^{2-}$ (**5a**) |
| | | *cis*-$[Re_6(\mu_3\text{-}S)_8Cl_4(mpy)_2]^{2-}$ (**5b**) |
| dmap | 9.7 | *trans*-$[Re_6(\mu_3\text{-}S)_8Cl_4(dmap)_2]^{2-}$ (**6a**) |
| | | *cis*-$[Re_6(\mu_3\text{-}S)_8Cl_4(dmap)_2]^{2-}$ (**6b**) |

## Experimental Section

**Materials.** $[Bu_4N]_3[Re_6(\mu_3\text{-}S)_8Cl_6]$ ($Bu_4N^+$ = tetra-*n*-butylammonium cation) was prepared according to the method in the literature.[38] $[Bu_4N]_2$[*trans*- and *cis*-$\{Re_6(\mu_3\text{-}S)_8Cl_4(cpy)_2\}$] (**2a** and **2b**, respectively) and $[Bu_4N]_2$[*trans*- and *cis*-$\{Re_6(\mu_3\text{-}S)_8Cl_4(py)_2\}$] (**4a** and **4b**, respectively) were prepared as described previously.[10] All ligands, pz, bpy, mpy, and dmap, were purchased from Wako Chemicals and used without further purification. $[Bu_4N]PF_6$ was recrystallized twice from ethanol, and acetonitrile for the electrochemical measurements was distilled under an argon atmosphere. For the photophysical measurements, spectrophotometric grade acetonitrile (Dotite) was dried over $CaH_2$ and distilled under an argon atmosphere. Other solvents were used without further distillation.

**Preparations of the Complexes. (a) $[Bu_4N]_2$[*trans*-$\{Re_6(\mu_3\text{-}S)_8Cl_4(pz)_2\}$] (1a) and $[Bu_4N]_2$[*cis*-$\{Re_6(\mu_3\text{-}S)_8Cl_4(pz)_2\}$] (1b).** $[Bu_4N]_3[Re_6(\mu_3\text{-}S)_8Cl_6]$ (0.300 g, 0.13 mmol) and pyrazine (208 mg, 2.6 mmol) were dissolved in 60 mL of DMF. The solution was refluxed for 3 h and then evaporated to ca. 1 mL. On addition of 20 mL of water, a red-brown solid was deposited. The solid was dissolved in dichloromethane, and the solution was passed through a silica gel column. From the red-brown products held on the top of the column, geometrical isomers **1a** and **1b** were separated as follows.

The first band was collected with 1/80 ethanol/dichloromethane, and the eluate was left for several days to allow for evaporation in air. The red-brown solid that deposited was filtered off, washed sequentially with water and a mixture of acetone and ether, and then dried in vacuo. Yield of the trans isomer **1a**: 0.050 g (18%). Absorption data

(26) Fedorov, V. E.; Tkachev, S. V.; Naumov, N. G.; Mironov, Yu. V.; Mironov, Yu. I. *Russ. J. Inorg. Chem. (Engl. Transl.)* **1998**, *43*, 1683−1693.
(27) Slougui, A.; Ferron, S.; Perrin, A.; Sergent, M. *J. Cluster Sci.* **1997**, *8*, 349−359.
(28) Fedorov, V. E.; Mironov, Yu. I.; Mironov, Yu. V.; Naumov, N. G.; Pek, U.-Kh.; Sin, S. Ch. *Russ. J. Inorg. Chem. (Engl. Transl.)* **1998**, *43*, 1916−1920.
(29) Simon, F.; Boubekeur, K.; Gabriel, J.-C. P.; Batail, P. *Chem. Commun.* **1998**, 845−846.
(30) Naumov, N. G.; Virovets, A. V.; Sokolov, M. N.; Artemkina, S. B.; Fedorov, V. E. *Angew. Chem., Int. Ed. Engl.* **1998**, *37*, 1943−1945.
(31) Beauvais, L. G.; Shores, M. P.; Long, J. R. *Chem. Mater.* **1998**, *10*, 3783−3786.
(32) Naumov, N. G.; Virovets, A. V.; Mironov, Yu. I.; Artemkina, S. B.; Fedorov, V. E. *Ukr. J. Chem.*, submitted for publication.
(33) Naumov, N. G.; Virovets, A. V.; Artemkina, S. B.; Naumov, D. Yu.; Howard, J. A.; Fedorov, V. E. Submitted for publication.
(34) Naumov, N. G.; Artemkina, S. B.; Virovets, A. V.; Fedorov, V. E. Unpublished work.
(35) Zheng, Z.; Holm, R. H. *Inorg. Chem.* **1997**, *36*, 5173−5178.
(36) Zheng, Z.; Long, J. R.; Holm, R. H. *J. Am. Chem. Soc.* **1997**, *119*, 2163-2171.
(37) Willer, M. W.; Long, J. R.; McLauchlan, C. C.; Holm, R. H. *Inorg. Chem.* **1998**, *37*, 328−333.
(38) Long, J. R.; McCarty, L. S.; Holm, R. H. *J. Am. Chem. Soc.* **1996**, *118*, 4603−4616.

(acetonitrile; $\lambda_{max}$/nm ($\epsilon$/$M^{-1}$ $cm^{-1}$)): 502 (190), 316 (9800), 269 (24 100), 237 (36 000), 222 (52 300). Anal. Calcd for $C_{40}H_{80}N_6S_8Cl_4Re_6$: C, 22.24; H, 3.73; N, 3.89; S, 11.87; Cl, 6.56. Found: C, 22.42; H, 3.68; N, 4.00; S, 11.92; Cl, 6.68. FAB-MS: $m/z$ = 2160 ($M^-$ − $Bu_4N$). $^1$H NMR ($CD_3CN$, 23 °C): $\delta$ 0.96 (t, 24H, $Bu_4N$), 1.35 (q, 16H, $Bu_4N$), 1.60 (q, 16H, $Bu_4N$), 3.07 (m, 16H, $Bu_4N$), 8.62 (d, 4H, $H_m$), 9.35 (d, 4H, $H_o$).

The second band was collected with 1/80 ethanol/dichloromethane, and the eluate was left for several days to allow for evaporation in air. The red-brown solid that deposited was collected, washed sequentially with water and ether, and then dried in vacuo. Yield of the cis isomer **1b**: 0.040 g (14%). Absorption data (acetonitrile; $\lambda_{max}$/nm ($\epsilon$/$M^{-1}$ $cm^{-1}$)): 516 (250), 270 (24 100), 237 (39 600), 220 (53 000). Anal. Calcd: same as **1a**. Found: C, 22.49; H, 3.66; N, 3.74; S, 11.91; Cl, 6.55. FAB-MS: $m/z$ = 2160. $^1$H NMR ($CD_3CN$, 23 °C): $\delta$ 0.96 (t, 24H, $Bu_4N$), 1.35 (q, 16H, $Bu_4N$), 1.60 (q, 16H, $Bu_4N$), 3.07 (m, 16H, $Bu_4N$), 8.65 (t, 4H, $H_m$), 9.44 (d, 4H, $H_o$).

**(b) $[Bu_4N]_2$[*trans*-{$Re_6(\mu_3\text{-}S)_8Cl_4(bpy)_2$}] (3a), $[Bu_4N]_2$[*cis*-{$Re_6(\mu_3\text{-}S)_8Cl_4(bpy)_2$}] (3b), and $[Bu_4N]$[*mer*-{$Re_6(\mu_3\text{-}S)_8Cl_3(bpy)_3$}] (3c).** $[Bu_4N]_3[Re_6(\mu_3\text{-}S)_8Cl_6]$ (0.300 g, 0.13 mmol) and 4,4′-bipyridine (0.404 g, 2.6 mmol) were dissolved in 60 mL of DMF. The solution was refluxed for 1 h and then evaporated to 5 mL in vacuo. On addition of 20 mL of water, a yellow-orange precipitate was formed, which was collected by filtration. The solid was dissolved in dichloromethane, and the solution was chromatographed on a silica gel column to obtain the geometrical isomers. Yellow-orange products were held on the top of the column. The first yellow-orange band eluted with 1/25 ethanol/dichloromethane gave a small amount of oily product, which was not identified.

The second band was eluted with 1/25 ethanol/dichloromethane, and the eluate was left for several days to allow for evaporation in air. The orange solid that deposited was filtered off, washed sequentially with water and a mixture of acetone and ether, and then dried in vacuo. Yield of the trans isomer **3a**: 0.030 g (10%). Absorption data (acetonitrile; $\lambda_{max}$/nm ($\epsilon$/$M^{-1}$ $cm^{-1}$)): 496 (sh, 430), 414 (2400), 324 (sh, 20 000), 274 (sh, 68 800), 248 (85 500), 224 (sh, 67 200). Anal. Calcd for $C_{52}H_{52}N_6S_8Cl_4Re_6$: C, 27.00; H, 3.84; N, 3.63; S, 11.69; Cl, 6.13. Found: C, 26.93; H, 3.36; N, 3.78; S, 11.47; Cl, 6.37. FAB-MS: $m/z$ = 2309. $^1$H NMR ($CD_3CN$, 23 °C): $\delta$ 0.96 (t, 24H, $Bu_4N$), 1.35 (q, 16H, $Bu_4N$), 1.60 (q, 16H, $Bu_4N$), 3.07 (m, 16H, $Bu_4N$), 7.59 (t, 8H, $H_m$), 8.73 (d, 4H, $H_o$), 9.45 (d, 4H, $H_o$).

The third band was eluted with 1/25 ethanol/dichloromethane, and the eluate was left for several days to allow for evaporation in air to dryness. The orange solid was washed sequentially with water and a mixture of acetone and ether and was then dried in vacuo. Yield of the cis isomer **3b**: 0.038 g (13%). Absorption data (acetonitrile; $\lambda_{max}$/nm ($\epsilon$/$M^{-1}$ $cm^{-1}$)): 505 (sh, 380), 413 (4400), 308 (sh, 25 300), 274 (sh, 51 300), 244 (87 500), 224 (sh, 69 900). Anal. Calcd: same as **3b**. Found: C, 27.89; H, 3.92; N, 3.76; S, 11.46; Cl, 6.34. FAB-MS: $m/z$ = 2311. $^1$H NMR ($CD_3CN$, 23 °C): $\delta$ 0.96 (t, 24H, $Bu_4N$), 1.35 (q, 16H, $Bu_4N$), 1.60 (q, 16H, $Bu_4N$), 3.07 (m, 16H, $Bu_4N$), 7.59 (t, 8H, $H_m$), 8.73 (d, 4H, $H_o$), 9.53 (d, 4H, $H_o$).

The fourth band was eluted with 1/20 ethanol/dichloromethane, and the eluate was evaporated to dryness. The residue was recrystallized by diffusing ether into the acetonitrile solution. The yellow-orange solid was collected by filtration, washed with a mixture of acetone and ether, and then dried in vacuo. Yield of **3c**: 0.014 g (5%). Absorption data (acetonitrile; $\lambda_{max}$/nm ($\epsilon$/$M^{-1}$ $cm^{-1}$)): 314 (21 300), 247 (65 500). Anal. Calcd for $C_{46}H_{60}N_7S_8Cl_3Re_6$: C, 25.22; H, 2.76; N, 4.48; S, 11.71; Cl, 4.85. Found: C, 24.45; H, 2.75; N, 4.85; S, 11.49; Cl, 4.51. FAB-MS: $m/z$ = 2191. $^1$H NMR ($CD_3CN$, 23 °C): $\delta$ 0.96 (t, 12H, $Bu_4N$), 1.35 (q, 8H, $Bu_4N$), 1.60 (q, 8H, $Bu_4N$), 3.07 (m, 8H, $Bu_4N$), 7.68 (t, 12H, $H_m$), 8.73 (d, 6H, $H_o$), 9.48 (d, 4H, $H_o$), 9.54 (d, 2H, $H_o$).

**(c) $[Bu_4N]_2$[*trans*-{$Re_6(\mu_3\text{-}S)_8Cl_4(mpy)_2$}] (5a) and $[Bu_4N]_2$[*cis*-{$Re_6(\mu_3\text{-}S)_8Cl_4(mpy)_2$}] (5b).** $[Bu_4N]_3[Re_6(\mu_3\text{-}S)_8Cl_6]$ (0.300 g, 0.13 mmol) and 4-methylpyridine (0.121 g, 1.3 mmol) was dissolved in 50 mL of DMF. The solution was refluxed for 1 h and then reduced to dryness in vacuo. On addition of 20 mL of water, a yellow-orange precipitate was formed. After filtration, the precipitate was dissolved in dichloromethane, and the solution was chromatographed on a silica gel column to separate the geometrical isomers. Yellow-orange products were held on the top of the column. The first and the second bands gave only small amounts of oily products, which were not identified.

The third band was collected with 1/6 acetonitrile/dichloromethane, and the eluate was left for several days to allow for evaporation. The yellow solid was filtered off, washed sequentially with water and a mixed solvent of acetone and ether, and then dried in vacuo. Yield of the trans isomer **5a**: 0.022 g (8%). Absorption data (acetonitrile; $\lambda_{max}$/nm ($\epsilon$/$M^{-1}$ $cm^{-1}$)): 422 (1010), 376 (sh, 2200), 268 (26 100), 240 (40 500), 224 (59 500). Anal. Calcd for $C_{44}H_{86}N_4S_8Cl_4Re_6$: C, 24.17; H, 3.96; N, 2.56; S, 11.73; Cl, 6.49. Found: C, 24.01; H, 3.78; N, 2.63; S, 11.71; Cl, 6.61. FAB-MS: $m/z$ = 2186. $^1$H NMR (DMSO-$d_6$, 23 °C): $\delta$ 0.93 (t, 24H, $Bu_4N$), 1.30 (q, 16H, $Bu_4N$), 1.57 (q, 16H, $Bu_4N$), 2.43 (s, 6H, $-CH_3$), 3.14 (m, 16H, $Bu_4N$), 7.34 (d, 4H, $H_m$), 9.09 (d, 4H, $H_o$).

The fourth band was collected with 1/6 acetonitrile/dichloromethane, and the eluate was left for several days to allow for evaporation to dryness. The yellow solid was washed sequentially with water and a mixed solvent of acetone and ether and then dried in vacuo. Yield of the cis isomer **5b**: 0.051 g (18%). Absorption data (acetonitrile; $\lambda_{max}$/nm ($\epsilon$/$M^{-1}$ $cm^{-1}$)): 424 (sh, 970), 376 (sh, 2300), 270 (25 600), 239 (43 300), 226 (57 800). Anal. Calcd: same as **5a**. Found: C, 24.21; H, 3.81; N, 2.73; S, 11.78; Cl, 6.47. FAB-MS: $m/z$ = 2186. $^1$H NMR (DMSO-$d_6$, 23 °C): $\delta$ 0.93 (t, 24H, $Bu_4N$), 1.30 (q, 16H, $Bu_4N$), 1.57 (q, 16H, $Bu_4N$), 2.44 (s, 6H, $CH_3$), 3.14 (m, 16H, $Bu_4N$), 7.34 (d, 4H, $H_m$), 9.15 (d, 4H, $H_o$).

**(d) $[Bu_4N]_2$[*trans*-{$Re_6(\mu_3\text{-}S)_8Cl_4(dmap)_2$}] (6a) and $[Bu_4N]_2${*cis*-{$Re_6(\mu_3\text{-}S)_8Cl_4(dmap)_2$}] (6b).** $[Bu_4N]_3[Re_6(\mu_3\text{-}S)_8Cl_6]$ (0.300 g, 0.13 mmol) and 4-(dimethylamino)pyridine (0.064 g, 0.52 mmol) were dissolved in 70 mL of DMF. The solution was refluxed for 15 min and then evaporated to 5 mL in vacuo. On addition of 20 mL of water, a yellow-orange precipitate was formed, which was collected by filtration and then dissolved in dichloromethane. The solution was chromatographed on a silica gel column to obtain the geometrical isomers. Yellow products were held on the top of the column. The first two bands gave only small amounts of the products and were discarded.

The third band was eluted with 1/6 acetonitrile/dichloromethane, and the eluate was left for several days to allow for evaporation. The yellow solid that was obtained was filtered off, washed sequentially with water and a mixed solvent of acetone and ether, and then dried in vacuo. Yield of the trans isomer **6a**: 0.018 g (6%). Absorption data (acetonitrile; $\lambda_{max}$/nm ($\epsilon$/$M^{-1}$ $cm^{-1}$)): 420 (1450), 310 (sh, 46 700), 281 (83 000), 243 (50 000), 224 (64 000). Anal. Calcd for $C_{46}H_{92}N_6S_8Cl_4Re_6$: C, 24.61; H, 4.13; N, 3.74; S, 11.43; Cl, 6.32. Found: C, 23.89; H, 3.87; N, 3.89; S, 10.88; Cl, 5.63. FAB-MS: $m/z$ = 2244. $^1$H NMR (DMSO-$d_6$, 23 °C): $\delta$ 0.93 (t, 24H, $Bu_4N$), 1.30 (q, 16H, $Bu_4N$), 1.57 (q, 16H, $Bu_4N$), 3.04 (s, 12H, $Bu_4N$), 3.14 (m, 16H, $Bu_4N$), 6.60 (d, 4H, $H_m$), 8.61 (d, 4H, $H_o$).

The fourth band was collected with 1/6 acetonitrile/dichloromethane, and the eluate was left for several days to allow for evaporation to dryness. The yellow solid was washed sequentially with water and a mixed solvent of acetone and ether and then dried in vacuo. Yield of the cis isomer **6b**: 0.034 g (13%). Absorption data (acetonitrile; $\lambda_{max}$/nm ($\epsilon$/$M^{-1}$ $cm^{-1}$)): 420 (1400), 278 (82 900), 244 (sh, 48 000), 224 (63 000). Anal. Calcd: same as **6a**. Found: C, 24.64; H, 4.02; N, 3.69; S, 11.43; Cl, 6.36. FAB-MS: $m/z$ = 2243. $^1$H NMR (DMSO-$d_6$, 23 °C): $\delta$ 0.93 (t, 24H, $Bu_4N$), 1.30 (q, 16H, $Bu_4N$), 1.57 (q, 16H, $Bu_4N$), 3.05 (s, 12H, $CH_3$), 3.14 (m, 16H, $Bu_4N$), 6.61 (d, 4H, $H_m$), 8.65 (d, 4H, $H_o$).

**Physical Measurements.** UV−visible absorption spectra were recorded on a Hitachi U3410 or U3000 spectrophotometer. Cyclic voltammetry was performed with a BAS-50W potentiostat and a software package. The working and counter electrodes were a glassy-carbon disk and a platinum wire, respectively. Cyclic voltammograms were recorded at a scan rate of 100 mV/s. The sample solutions (ca. 1 mM) in 0.1 M [*n*-$Bu_4N$]$PF_6$/acetonitrile were deoxygenated with a stream of argon gas. The reference electrode was Ag/AgCl, against which the half-wave potential of $Fc^+$/Fc ($E_{1/2}$($Fc^{+/0}$)) was 0.43 V. The $^1$H NMR spectra were obtained at 270.05 MHz with a JEOL JNM-EX

**Table 1.** Crystallographic Data for $[Bu_4N]_2[trans\text{-}\{Re_6(\mu_3\text{-}S)_8Cl_4(pz)_2\}]$ (**1a**)

| | |
|---|---|
| empirical formula | $C_{40}H_{80}N_6S_8Cl_4Re_6$ |
| fw | 2160.65 |
| $T$/K | 296 |
| $\lambda$/Å | 0.710 69 |
| cryst syst | orthorhombic |
| space group | *Cmca* (No. 64) |
| color | red |
| $Z$ | 4 |
| $a$/Å | 19.560(5) |
| b/Å | 16.257(4) |
| c/Å | 19.050(4) |
| V/Å$^3$ | 6057(4) |
| $D_{calc}$/g cm$^{-3}$ | 2.369 |
| $\mu$(Mo K$\alpha$)/cm$^{-1}$ | 125.86 |
| $R$,[a] $R_w$[b]/% | 3.3, 4.0 |
| GOF | 1.82 |

[a] $R = \sum||F_o| - |F_c||/\sum|F_o|$. [b] $R_w = [\sum w(|F_o| - |F_c|)^2/\sum w|F_o|^2]^{1/2}$.

270 spectrometer. All peaks were referenced to the methyl signals of TMS at $\delta = 0$. Corrected emission spectra were obtained by using a red-sensitive photodetector (Hamamatsu PMA-11, model C5966-23) and an Nd:YAG Laser (Continuum Surelite) at 355 nm excitation. The instrumental responses of the system were corrected by using a software package for the detector. Lifetime measurements were conducted by using a streak camera (Hamamatsu C4334) as a detector. Emission quantum yields were estimated by using $[n\text{-}Bu_4N]_2[Mo_6(\mu_3\text{-}Cl)_8Cl_6]$ ($\phi_{em} = 0.19$)[39] as a standard. Sample solutions were deaerated thoroughly by purging with an Ar gas stream for 15 min prior to the experiments and then sealed in their cells.

**X-ray Structural Determinations.** A single-crystal of **1a** was sealed in a glass capillary. X-ray data were collected at ambient temperature on a Rigaku AFC5R diffractmeter with graphite-monochromated Mo K$\alpha$ radiation. Unit cell parameters were obtained by least-squares refinement of 25 reflections ($25° \le 2\theta \le 30°$). Decay corrections were based on the measured intensities of reflections monitored periodically throughout the course of the data collection. The crystal showed no significant decay. The data were corrected for Lorentz and polarization effects, and an absorption correction ($\psi$ scans) was applied to data set. The crystal structure was solved by direct methods (SIR92).[40] Atomic coordinates and anisotropic thermal parameters of the non-hydrogen atoms were refined by full-matrix least-squares calculations. The hydrogen atoms on the pyrazine ligands were placed at calculated positions and were refined using a model with an isotropic thermal parameter 1.2 times that of the attached carbon atom. All calculations were performed using TEXSAN.[41] Crystallographic data are listed in Table 1.

## Results and Discussion

**Preparation and Characterization of the Complexes.** In a previous paper, we reported the preparation of a series of octakis($\mu_3$-sulfido)hexarhenium(III) complexes of mixed chloro−pyridine (py) and chloro−4-cyanopyridine (cpy) terminal ligands, $[Re_6(\mu_3\text{-}S)_8Cl_{6-n}(L)_n]^{(4-n)-}$ (L = py, $n = 2-4$; L = cpy, $n = 2$), by the reaction of the $Re^{III}_5Re^{IV}$ complex $[Re_6(\mu_3\text{-}S)_8Cl_6]^{3-}$ with py or cpy in DMF solution with varied ratios of the reactants and reaction times.[10] The new complexes, $[Re_6(\mu_3\text{-}S)_8Cl_4(L)_2]^{2-}$ (L = pz, bpy, mpy, dmap), were prepared by synthetic procedures similar to those reported for their py and cpy analogues. The reaction is not a simple terminal ligand substitution of $[Re_6(\mu_3\text{-}S)_8Cl_6]^{3-}$ because simultaneous reduction of the hexarhenium core takes place during the reaction. Nevertheless, the ease with which substitution for the terminal chloride ligands occurs depends significantly on the incoming ligand, more basic N-heterocycles tending to require shorter reaction times and smaller excesses over the hexarhenium reactant. Treatment of $[Re_6(\mu_3\text{-}S)_8Cl_6]^{3-}$ with a 20-fold molar excess of pz gave **1a** and **1b** under reflux for 3 h. Only 1 h of reflux was sufficient to obtain **3a** and **3b** from the reaction mixture of $[Re_6(\mu_3\text{-}S)_8Cl_6]^{3-}$ and a 20-fold excess of bpy. The mpy complexes **4a** and **4b** were prepared under 1 h reflux of the reaction mixture with 10 equiv of the ligand. In the case of the most basic ligand dmap, **6a** and **6b** were obtained after only 15 min and 1.2 h of reflux with 4 and 2.5 equiv of the ligand, respectively. Two geometrical isomers, trans and cis, of all the complexes were separated by silica gel chromatography by eluting with mixed solvents of dichloromethane and increasing amounts of ethanol or acetonitrile. It was reported previously that, for the py and cpy complexes, the trans isomers eluted first, followed by the corresponding cis isomers, the assignment being confirmed by the X-ray structural analyses.[10] We have assigned the trans isomers of all the complexes to the compounds eluted first (vide infra).

Characterization of the complexes, including the assignment of the isomers, was performed mainly on the basis of the $^1$H NMR spectra and, in one instance, the X-ray crystallographic determination. All signals of the complexed ligands were observed at lower fields than those of the free ligands in the range of diamagnetic metal complexes, supporting the $Re^{III}_6$ oxidation state for all the complexes. The spectra of the $CD_3CN$ solutions remained unchanged after a week at room temperature, suggesting that ligand dissociation from the $[Re^{III}_6(\mu_3\text{-}S)_8]^{2+}$ core does not take place. As to the spectra of the geometrical isomers, we have shown previously for the py and cpy complexes that the $H_\alpha$ signals of the trans isomers were observed at higher fields than those of the corresponding cis isomers. We found that, for the present pz, bpy, mpy, and dmap complexes, the isomers eluted first by silica gel chromatography always show their $H_\alpha$ signals at higher magnetic fields than the isomers eluted later. Moreover, X-ray structural analysis confirmed that the first eluted isomer, **1a**, of the pz complexes has a trans geometrical configuration (vide infra) (Figure 1). By considering all these facts, we conclude that the isomers eluted first and having $H_\alpha$ signals in upper magnetic fields are the trans ones for all of the N-heterocyclic ligands.

The pz and bpy ligands have two nitrogen coordination sites, but they coordinate to the $Re_6$ center as monodentate ligands. In addition to being indicated by X-ray structural analysis, the monodentate coordination of **1a** is supported by its $^1$H NMR spectra, which clearly show that the two nitrogen sites of these ligands are inequivalent. One set of the signals appears in the region of coordinated pyridyl groups, whereas the other set is in the region of the corresponding free ligand. The mer configuration of the $(bpy)_3$ complex **3c** was confirmed by the splitting of the $H_\alpha$ signal of the coordinated pyridine ring in a 2:1 ratio as well as the observation of the $H_\alpha$ signal from the uncoordinated pyridyl ring in the free ligand region.

For the hexahalogeno complex $[Re_6(\mu_3\text{-}S)_8X_6]^{4-}$ ($X^-$ = halide ion), there are distinct absorption peaks at ca. 430 nm (the chloro complex shows a peak at 436 nm in acetonitrile that shifts to longer wavelengths as X becomes heavier). This band was assigned to LMCT ($X^-$ to Re) transitions.[38] The present complexes containing N-heterocycles show less defined absorption in the region 300−450 nm due to overlap of possible metal-to-N-heterocyclic ligand charge transfer with the LMCT transition, except for **5** and **6**, for which the LMCT bands are

(39) Maverick, A. W.; Najdionek, J. S.; MacKenzie, D.; Nocera, D. G.; Gray, H. B. *J. Am. Chem. Soc.* **1983**, *105*, 1878−1882.
(40) Altomare, A.; Cascarano, G.; Giacovazzo, C.; Guagliari, A.; Burla, M. C.; Polidori, G.; Camalli, M. *J. Appl. Crystallogr.* **1994**, *27*, 435.
(41) *TEXAN: Single-Crystal Structure Analysis Package*; Molecular Structure Corp.: The Woodlands, TX, 1992.

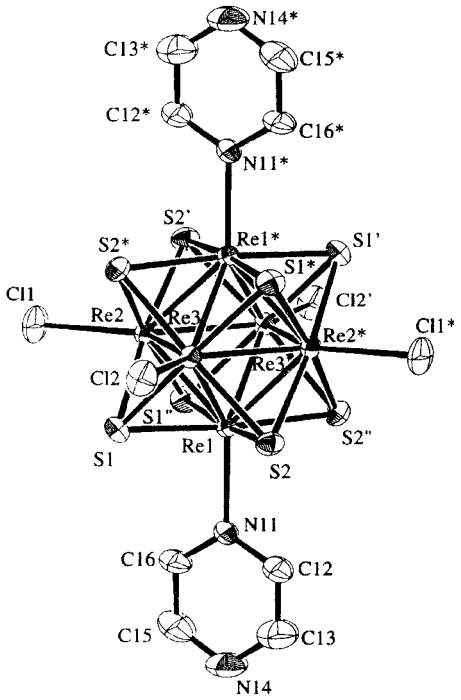


**Figure 1.** ORTEP drawing showing the complex anion and numbering scheme for $[Bu_4N]_2[trans\text{-}\{Re_6(\mu_3\text{-}S)_8Cl_4(pz)_2\}]$ (**1a**). Ellipsoids are drawn at the 50% probability level, and hydrogen atoms are omitted for clarity.

**Table 2.** Selected Bond Distances (Å) and Angles (deg) for $[Bu_4N]_2[trans\text{-}\{Re_6(\mu_3\text{-}S)_8Cl_4(pz)_2\}]$ (**1a**)

| | | | |
|---|---|---|---|
| Re−Re | 2.5886(8)−2.6008(6) | Re−S−Re | 65.19(7)−65.41(7) |
| av | 2.5942 | av | 65.27 |
| Re−S | 2.394(3)−2.418(3) | S−Re−S | 172.7(1)−174.5(1) |
| av | 2.405 | av | 173.5 |
| Re−N | 2.21(1) | S−Re−S | 89.20(9)−90.35(9) |
| Re−Cl | 2.419(4), 2.421(4) | av | 89.8 |
| av | 2.420 | Re−Re−N | 134.6(3)−135.0(3) |
| Re−Re−Re | 89.50(3)−90.50(3) | av | 134.8 |
| av | 90.00 | Re−Re−Cl | 134.7(1)−135.7(1) |
| Re−Re−Re | 59.80(2)−60.27(2) | av | 135.2 |
| av | 60.00 | | |

still observable at 420−430 nm. A band observed at ca. 413 nm for **3a** and **3b** would involve the contribution from the MLCT transition to the bpy ligands, since the intensity is considerably higher than that of the LMCT transition ($Cl^-$ to Re) of other $Re_6$ complexes. It should be noted that complexes **1**−**3**, which contain N-hetrocyclic ligands having low-lying $\pi^*$ orbitals, show absorption shoulders at 495−520 nm, whereas complexes **4**−**6** show no shoulders.

**X-ray Structure of $[Bu_4N]_2[trans\text{-}\{Re_6(\mu_3\text{-}S)_8Cl_4(pz)_2\}]$.** Single crystals suitable for X-ray crystallography were obtained by slow diffusion of ether into the acetonitrile solution of $[Bu_4N]_2[trans\text{-}\{Re_6(\mu_3\text{-}S)_8Cl_4(pz)_2\}]$ (**1a**). The ORTEP drawing of the anion of **1a** is shown in Figure 1. Table 2 summarizes selected bond lengths and angles. Each rhenium atom is located at vertex positions of the $Re_6$ octahedron. Two rhenium atoms coordinated by pz ligands are orientated in mutually trans positions. The Re−Re and Re−S distances are in the ranges 2.5906(8)−2.6008(6) and 2.395(3)−2.418(3) Å, respectively. The Re−N(pz) distance is 2.21(1) Å. All distances and angles are in the ranges of the values observed for py and cpy analogues.

**Electrochemical Studies.** Electrochemical properties of the new series of complexes were investigated by cyclic and differential-pulse voltammetries in 0.1 M $[Bu_4N]PF_6$/acetonitrile solutions. Electrochemical data for all of the complexes are summarized in Table 3. The cyclic voltammograms of *cis*-$[Re_6(\mu_3\text{-}S)_8Cl_4(pz)_2]^{2-}$ and *cis*-$[Re_6(\mu_3\text{-}S)_8Cl_4(dmap)_2]^{2-}$ are shown in Figure 2.

**Table 3.** Redox Potentials of the New Complexes in 0.1 M $[Bu_4N]PF_6/CH_3CN$

| | $E_{1/2}{}^a$/V vs Ag/AgCl ($\Delta E_p{}^b$) | |
|---|---|---|
| | $Re^{III}{}_6/Re^{III}{}_5Re^{IV}$ | $L^{\bullet-}/L$ |
| $[Bu_4N]_2[trans\text{-}\{Re_6(\mu_3\text{-}S)_8Cl_4(pz)_2\}]$ (**1a**) | +0.86 (70) | −1.34, −1.45 |
| $[Bu_4N]_2[cis\text{-}\{Re_6(\mu_3\text{-}S)_8Cl_4(pz)_2\}]$ (**1b**) | +0.86 (70) | −1.33, −1.47 |
| $[Bu_4N]_2[trans\text{-}\{Re_6(\mu_3\text{-}S)_8Cl_4(cpy)_2\}]$ (**2a**) | +0.83 (60) | −1.19, −1.28 |
| $[Bu_4N]_2[cis\text{-}\{Re_6(\mu_3\text{-}S)_8Cl_4(cpy)_2\}]$ (**2b**) | +0.83 (60) | −1.18, −1.29 |
| $[Bu_4N]_2[trans\text{-}\{Re_6(\mu_3\text{-}S)_8Cl_4(bpy)_2\}]$ (**3a**) | +0.79 (60) | −1.45 ($2e^-$), −1.96 ($2e^-$) |
| $[Bu_4N]_2[cis\text{-}\{Re_6(\mu_3\text{-}S)_8Cl_4(bpy)_2\}]$ (**3b**) | +0.79 (60) | −1.44 ($2e^-$), −1.94 ($2e^-$) |
| $[Bu_4N]_2[trans\text{-}\{Re_6(\mu_3\text{-}S)_8Cl_4(py)_2\}]$ (**4a**) | +0.77 (60) | |
| $[Bu_4N]_2[cis\text{-}\{Re_6(\mu_3\text{-}S)_8Cl_4(py)_2\}]$ (**4b**) | +0.77 (60) | |
| $[Bu_4N]_2[trans\text{-}\{Re_6(\mu_3\text{-}S)_8Cl_4(mpy)_2\}]$ (**5a**) | +0.75 (60) | |
| $[Bu_4N]_2[cis\text{-}\{Re_6(\mu_3\text{-}S)_8Cl_4(mpy)_2\}]$ (**5b**) | +0.75 (60) | |
| $[Bu_4N]_2[trans\text{-}\{Re_6(\mu_3\text{-}S)_8Cl_4(dmap)_2\}]$ (**6a**) | +0.68 (60) | |
| $[Bu_4N]_2[cis\text{-}\{Re_6(\mu_3\text{-}S)_8Cl_4(dmap)_2\}]$ (**6b**) | +0.68 (60) | |

[a] $E_{1/2} = (E_{pa} + E_{pc})/2$, where $E_{pa}$ and $E_{pc}$ are the anodic and cathodic peak potentials, respectively; values in volts. [b] $\Delta E_p = E_{pa} - E_{pc}$; values in millivolts.

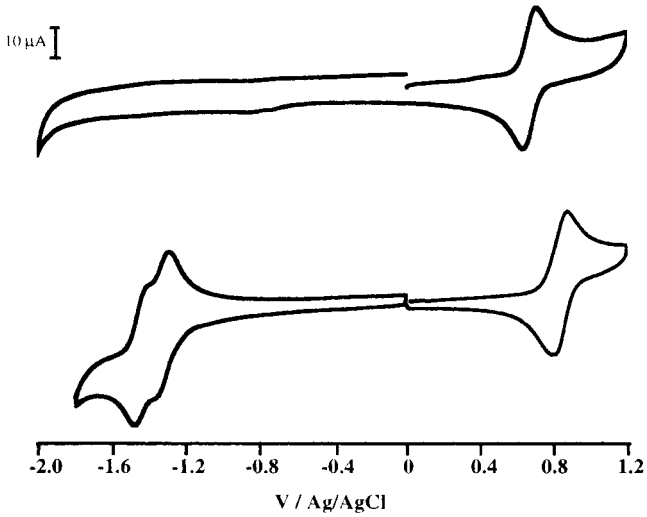


**Figure 2.** Cyclic voltammograms of $[Bu_4N]_2[cis\text{-}\{Re_6(\mu_3\text{-}S)_8Cl_4(dmap)_2\}]$ (upper) and $[Bu_4N]_2[cis\text{-}\{Re_6(\mu_3\text{-}S)_8Cl_4(pz)_2\}]$ (lower) in 0.1 M $[Bu_4N]PF_6/CH_3CN$ solution. Scan rate = 100 mV/s.

**(a) Dependence of $E_{1/2}$ for the $Re^{III}{}_6/Re^{III}{}_5Re^{IV}$ Couple on Terminal N-Heterocyclic Ligands.** All of the complexes **1**−**6**, including geometrical isomers, exhibit a reversible $Re^{III}{}_6/Re^{III}{}_5Re^{IV}$ wave. The one-electron nature of the wave has been confirmed coulometrically for complex **2a**. No difference in the $Re^{III}{}_6/Re^{III}{}_5Re^{IV}$ redox potentials is observed between cis and trans isomers for a given N-heterocyclic ligand. The $E_{1/2}$ values for the $Re^{III}{}_6/Re^{III}{}_5Re^{IV}$ couple are significantly more positive than that for $[Re_6(\mu_3\text{-}S)_8Cl_6]^{4-}$,[38] indicating that the ground state of the hexarhenium core is stabilized by the N-heterocyclic ligands. Within a series of *trans*- or *cis*-$[Re_6(\mu_3\text{-}S)_8Cl_4(L)_2]^{2-}$ complexes, $E_{1/2}$ becomes more positive in the order L = dmap < mpy < py < bpy < cpy < pz, suggesting that the coordination of electron-withdrawing groups makes the $[Re_6(\mu_3\text{-}S)_8]^{2+}$ core more difficult to oxidize. Figure 3 shows a good linear correlation between the $E_{1/2}$ and the p$K_a$ values of the N-heterocyclic ligands. Linear regression analysis of the plot gives eq 1.

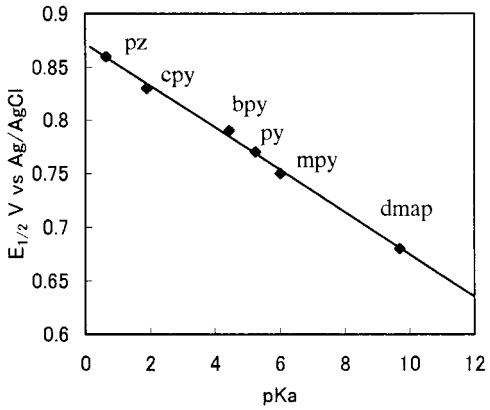


**Figure 3.** Correlation between the p$K_a$ of the free ligands and the redox potential of the complexes.

$$E_{1/2} = 0.8737 - 0.0197(\mathrm{p}K_a) \qquad R = 0.99 \qquad (1)$$

Clearly the $\sigma$ electrons of the N-heterocyclic ligands affect the HOMO levels of the rhenium clusters. The correlation should allow us to tune the redox potential of the $Re^{III}_6/Re^{III}_5Re^{IV}$ couple of the $[Re_6(\mu_3\text{-}S)_8]^{2+}$ core by choosing an N-heterocyclic ligand with an appropriate p$K_a$.

**(b) Ligand−Ligand Redox Interactions.** The free ligands pz and cpy exhibit a one-electron reduction wave at $E_{pc} = -2.1$ and $E_{1/2} = -1.79$ V vs Ag/AgCl, respectively. As shown in Figure 2, reversible two-step one-electron redox waves are observed for complexes **1a**, **1b**, **2a**, and **2b** in the range from −1.2 to −1.5 V vs Ag/AgCl. These waves were assigned to ligand-centered redox processes $((L)_2 \rightarrow (L^{\bullet-})(L)$ and $(L^{\bullet-})(L) \rightarrow (L^{\bullet-})_2$; L = pz, cpy), since complexes **4**−**6** show no redox waves in the negative potential region up to −2.0 V. Figure 4 shows the cyclic voltammograms of the bpy complexes **3a** and **3b**. These complexes show two-step redox waves for the reduction of the bpy ligands at ca. −1.44 and −1.96 V. The first and the second ligand reduction waves of complexes **3a** and **3b** are assigned to $(bpy)_2 \rightarrow (bpy^{\bullet-})_2$ and to $(bpy^{\bullet-})_2 \rightarrow (bpy^{2-})_2$, respectively. The first reduction wave of the free bpy ligand was observed at $E_{1/2} = -1.89$ V vs Ag/AgCl in 0.1 M $[Bu_4N]PF_6$/acetonitrile. The second reduction wave was not observed up to −2.2 V. Thus, the ligand redox potentials shift to positive potentials by at least 0.6 − 0.7 V from those of the free ligand. Since only the ligand-reduction waves were observed, the LUMOs of the pz, bpy, and cpy complexes must be ligand oriented. For complexes **4**−**6**, it is not clear whether the LUMOs are metal or ligand centered, as no reduction waves was observed.

Now we discuss further the splitting of the reduction waves of the two ligands coordinated to the $Re_6(\mu_3\text{-}S)_8$ core. Figure 5 shows the differential-pulse voltammograms of the ligand-reduction processes for the six complexes **1a**, **1b**, **2a**, **2b**, **3a**, and **3b**. Except for **3a** and **3b**, splitting of the ligand redox wave is clear. The extent of the splitting ($\Delta E_{1/2}$) is correlated with the comproportionation constant $K_c$, which is equal to $[(L^{\bullet-})(L)]^2/[(L)_2][(L^{\bullet-})_2]$.[42]

$$K_c = \exp(F\Delta E_{1/2}/RT) \qquad (F = \text{Faraday constant}) \quad (2)$$

The $\Delta E_{1/2}$ and $K_c$ values thus obtained are 120 mV and 107 for **1a**, 140 mV and 232 for **1b**, 90 mV and 34 for **2a**, and 110 mV and 72 for **2b**, respectively. The largest peak separation is found for **1b**. It is seen that a cis isomer tends to show larger splitting than the corresponding trans isomer. Splitting of the ligand-reduction waves for **3a** and **3b** is not obvious. The differential-pulse voltammetric waves for **3b** is broader than that for **3a**, however, and the $\Delta E_{1/2}$ values must be larger for the cis isomer **3a**.

(42) Richardson, D. E.; Taube, H. *Inorg. Chem.* **1981**, *20*, 1278−1285.

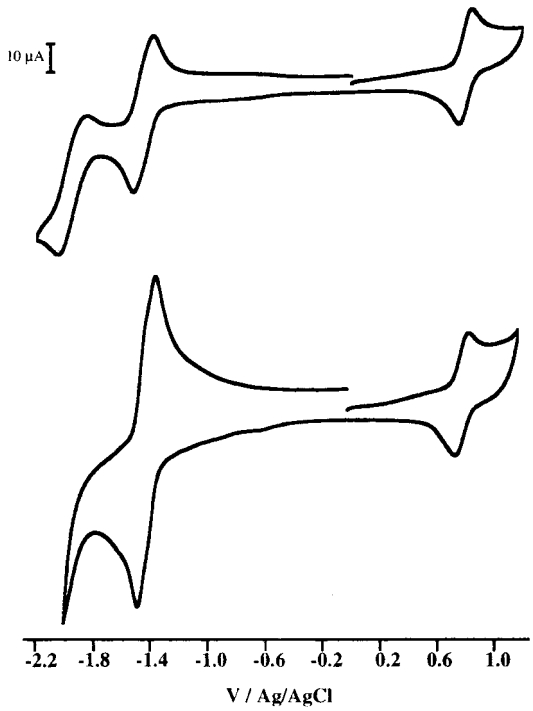


**Figure 4.** Cyclic voltammogram of $[Bu_4N]_2[trans\text{-}\{Re_6(\mu_3\text{-}S)_8Cl_4(bpy)_2\}]$ in 0.1 M $[Bu_4N]PF_6/CH_3CN$ solution (upper) and that after the addition of a few drops of water (lower). Scan rate = 100 mV/s.

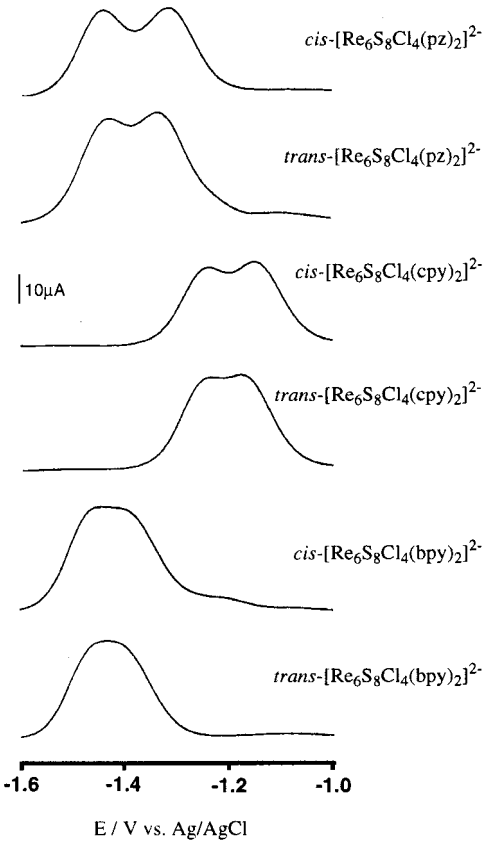


**Figure 5.** Differential-pulse voltammograms of the ligand-reduction waves in 0.1 M $[Bu_4N]PF_6/CH_3CN$ solution. Scan rate = 20 mV/s.

**Scheme 1**

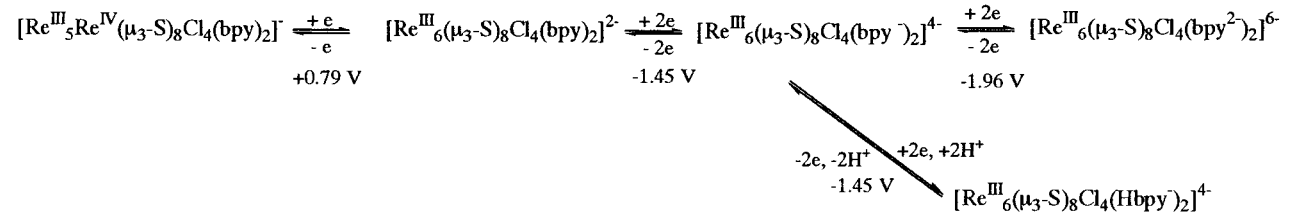


Two main factors controlling the splitting of a ligand-reduction wave in metal complexes were pointed out by Vlcek, i.e., electrostatic repulsions between ligands and metal-mediated ligand−ligand electronic interactions.[43] The electrostatic repulsion is unlikely to be important in the present complexes, particularly in the case of trans isomers, where the two ligands are separated by three Re atoms and are too far apart to have effective through-space interactions. It is more likely that an electronic interaction through the $[Re_6(\mu_3\text{-}S)_8]^{2+}$ core is responsible for the observed splitting of the ligand-reduction waves. For some oxo-centered trinuclear ruthenium(III) complexes, redox interactions of the three N-methyl-4,4′-bipyridinium ligands are shown to be mediated by vacant $\pi^*$ orbitals composed of metal d$\pi$ and oxo p$\pi$ orbitals,[44,45] as the trirhodium(III) analogue which has a filled $\pi^*$ orbital shows no redox interaction.[44] In the case of the $Re_6(\mu_3\text{-}S)_8$ core, the d electrons of Re(III) may be used mainly for Re−Re $\sigma$ bonding and the vacant d orbitals may be available for the ligand interactions.[2,7,46] The low-lying $\pi^*$ orbital of pz may be closer to unoccupied metal d orbitals than that of cpy, so that the electronic interaction is stronger for pz than for cpy. The fact that the interaction of the cis isomer is stronger than that of the corresponding trans isomer may suggest that the electrochemical interactions decrease as the number of spacer Re atoms between the two ligands increases from two (cis) to three (trans). The interactions between the bpy ligands of complexes **3a** and **3b** are weaker although their redox potentials are not significantly different from those of **1** and **2**. For Creutz−Taube type dinuclear complexes, it is known that the bridging 4,4′-bipyridine ligand is less interactive because of twisting of its two aromatic rings.[47] It is possible that similar twisting of the two aromatic rings would be responsible for the absence of significant splitting of the ligand-reduction waves of **3a** and **3b**.

**(c) Proton-Coupled Electron Transfer of the 4,4′-Bipyridine Complexes.** It was found that the second ligand-reduction waves of the bpy complexes **3a** and **3b** in acetonitrile are very sensitive to moisture. The redox waves observed at $E_{1/2} = -1.94$ V (cis) and −1.96 V (trans) in the freshly prepared solutions shift to positive potentials on standing, while other redox waves are unaffected. Addition of a few drops of water to the solutions causes a more drastic change, the second reduction wave being coalesced with the first one (originally at −1.44 and −1.45 V for the cis and the trans isomers, respectively) to give a reversible one-step four-electron wave (per one complex) centered at −1.44 V (Figure 4) (small splitting of the wave is noted, possibly due to the ligand−ligand interaction (vide supra)). This observation is reminiscent of the behavior of the oxo-bridged diruthenium complex $[Ru_2(\mu\text{-}O)(\mu\text{-}CH_3COO)(2,2'\text{-bipyridine})_2(1\text{-methylimidazole})_2]^{2+}$, where addition of the weak proton donor imidazole ($pK_a = 14.4$) caused the redox wave $Ru^{II}Ru^{II}/Ru^{II}Ru^{III}$ to shift positively, coalescing with the $Ru^{II}Ru^{III}/Ru^{III}Ru^{III}$ wave to give an apparent one-step two-electron wave.[48] This is explained by protonation of the oxide bridge at the $Ru^{II}Ru^{II}$ stage but not at the $Ru^{II}Ru^{III}$ stage to cause the shift of only the $Ru^{II}Ru^{II}/Ru^{II}Ru^{III}$ wave.

We added the weak proton donor imidazole to the acetonitrile solutions of **3a** and **3b**. Coalescence of the ligand-reduction waves was again observed. Selective protonation at $bpy^{2-}$ but not at $bpy^{\bullet-}$ by imidazole occurred, so that the more positive $Hbpy^-/Hbpy^\bullet$ wave was observed rather than that of $bpy^{2-}/bpy^{\bullet-}$. The necessary condition to observe the coalescence is that the redox potential of the $Hbpy^-/Hbpy^\bullet$ process is equal to or more positive than that of the $bpy^{2-}/bpy^{\bullet-}$ process. The processes are summarized in Scheme 1.

Estimation of the $pK_a$ values of the coordinated bpy of $[Re_6(\mu_3\text{-}S)_8Cl_4(bpy)_2]^{2-}$ was hampered by precipitation of the protonated species. Addition of a strong acid (*p*-toluenesulfonic acid) caused precipitation of both isomers. The precipitation, which was reversed upon addition of triethylamine, may be caused by the formation of a neutral species, $Re_6(\mu_3\text{-}S)_8Cl_4(Hbpy)_2$, upon protonation. Neutral hexarhenium complexes such as $Re_6(\mu_3\text{-}S)_8Cl_2(py)_4$ are often less soluble. The reported $pK_a$ values for coordinated 4,4′-bipyridines in $[Ru(NH_3)_5(bpy)]^{2+}$ [49] and $ReX(CO)_3(bpy)_2$ (X = Cl, Br, I)[50] fall within a range of 4−4.5. The $pK_a$ values for the coordinated bpy ligands in $[Re_6(\mu_3\text{-}S)_8Cl_4(bpy)_2]^{2-}$ would be similar to those of the mononuclear complexes. When 4,4′-bipyridine is reduced, the $pK_a$ value should increase. The $pK_a$ values of the one-electron-reduced bpy ligand may be approximated from the $pK_a$ values of the charge-transfer-excited state of some bpy complexes where the formation of $bpy^{\bullet-}$ is assumed. The values for the excited states of $[Ru(NH_3)_5(bpy)]^{2+}$ [49] and $ReX(CO)_3(bpy)_2$[50] were estimated to be $11.1 \pm 0.1$ and ca. 13.7, respectively. The $pK_a$ values of the two-electron-reduced $bpy^{2-}$ ligands in $[Re_6(\mu_3\text{-}S)_8Cl_4(bpy^{2-})_2]^{6-}$ would be even larger, and proton transfer from imidazole and water is very reasonable.

**Luminescence of the Complexes.** All of the complexes are luminescent in acetonitrile at room temperature. Table 4 summarizes the photophysical data for **1a**, **1b**, **3a**, **3b**, **5a**, and **5b** together with those for **4a**, **4b**, and *mer*-$[Re_6(\mu_3\text{-}S)_8Cl_3(py)_3]^-$ (**7**) at 298 K. It is clear that the emission characteristics are significantly different between the group of py and mpy complexes (**4a**, **4b**, **5a**, **5b**, and **7**) and that of bpy and pz complexes (**1a**, **1b**, **3a**, and **3b**). The latter group of the complexes show significantly smaller $\phi_{em}$ (0.0010−0.0017) and $\tau_{em}$ (0.013−0.029 $\mu$s) values and larger $\lambda_{em}$ values (765−785

(43) Vlcek, A. A. *Coord. Chem. Rev.* **1982**, *42*, 39−62.
(44) Abe, M.; Sasaki, Y.; Yamada, Y.; Tsukahara, K.; Yano, S.; Ito, T. *Inorg. Chem.* **1995**, *34*, 4490−4498.
(45) Abe, M.; Sasaki, Y.; Yamada, Y.; Tsukahara, K.; Yano, S.; Yamaguchi, T.; Tominaga, M.; Taniguchi, I.; Ito, T. *Inorg. Chem.* **1996**, *35*, 6724−6734.
(46) Honda, H.; Tanaka, K.; Noro, T.; Miyoshi, E. Private communications.
(47) Creutz, C. *Prog. Inorg. Chem.* **1983**, *30*, 1.
(48) Kikuchi, A.; Fukumoto, T.; Umakoshi, K.; Sasaki, Y.; Ichimura, A. *J. Chem. Soc., Chem. Commun.* **1995**, 2125−2126.
(49) Lavallee, D. K.; Fleischer, E. B. *J. Am. Chem. Soc.* **1972**, *94*, 2583−2599.
(50) Giordano, P. J.; Wrighton, M. S. *J. Am. Chem. Soc.* **1979**, *101*, 2888−2897.

**Table 4.** Photophysical Data for the Hexarhenium(III) Clusters in $CH_3CN$ at 298 K

| complex | $\lambda_{em}$/nm | $\phi_{em}$ | $\tau_{em}/\mu$s |
|---|---|---|---|
| $[Re_6(\mu_3\text{-}S)_8Cl_6]^{4-}$ [a] | 770 | 0.039 | 6.3 |
| $[Re_6(\mu_3\text{-}S)_8Br_6]^{4-}$ [a] | 780 | 0.018 | 5.4 |
| $[Re_6(\mu_3\text{-}S)_8I_6]^{4-}$ [a] | 800 | 0.015 | 4.4 |
| $[Re_6(\mu_3\text{-}S)_8(CN)_6]^{4-}$ [b] | 720 | 0.056 | 11.2 |
| [*trans*-$\{Re_6(\mu_3\text{-}S)_8Cl_4(pz)_2\}]^{2-}$ | 782 | 0.0017 | 0.029, 0.013[c] |
| [*cis*-$\{Re_6(\mu_3\text{-}S)_8Cl_4(pz)_2\}]^{2-}$ | 785 | 0.0010 | 0.021 |
| [*trans*-$\{Re_6(\mu_3\text{-}S)_8Cl_4(bpy)_2\}]^{2-}$ | 763 | 0.0013 | 0.019 |
| [*cis*-$\{Re_6(\mu_3\text{-}S)_8Cl_4(bpy)_2\}]^{2-}$ | 768 | 0.0011 | 0.013 |
| [*trans*-$\{Re_6(\mu_3\text{-}S)_8Cl_4(py)_2\}]^{2-}$ | 750 | 0.033 | 4.5 |
| [*cis*-$\{Re_6(\mu_3\text{-}S)_8Cl_4(py)_2\}]^{2-}$ | 745 | 0.042 | 5.1 |
| [*mer*-$\{Re_6(\mu_3\text{-}S)_8Cl_3(py)_3\}]^{-}$ | 740 | 0.045 | 5.9 |
| [*trans*-$\{Re_6(\mu_3\text{-}S)_8Cl_4(mpy)_2\}]^{2-}$ | 749 | 0.031 | 4.2 |
| [*cis*-$\{Re_6(\mu_3\text{-}S)_8Cl_4(mpy)_2\}]^{2-}$ | 745 | 0.057 | 6.2 |

[a] Reference 8. [b] Reference 9. [c] The decay was fitted by a double exponential curve.

nm) compared to the corresponding values for the former complexes (0.031−0.057, 4.2−6.2 $\mu$s, and 740−750 nm, respectively). The influence of geometrical isomerism appears to be insignificant. Clear trends in the photophysical data for the cis and trans isomers are observed, however, which are in opposite directions for the two groups. Thus, for the py and mpy complexes, $\phi_{em}$ and $\tau_{em}$ are smaller and $\lambda_{em}$ is shorter for the trans isomer, while for the pz and bpy complexes the trends are in the opposite direction.

On the basis of the photophysical data for two series of hexarhenium(III) complexes, $[Re_6(\mu_3\text{-}S)_8X_6]^{4-}$ (X = Cl, Br, I) and $[Re_6(\mu_3\text{-}E)_8(CN)_6]^{4-}$ (E = S, Se, Te), it has been suggested that the photoemissive excited state is largely localized on the $Re_6E_8$ core.[8,9] The pz, bpy, and cpy complexes all show ligand-centered-redox waves in the region −1.2 to −1.5 V, indicating that the LUMOs of these complexes are ligand centered. Thus the emissive excited state could be oriented at the ligand-centered $\pi^*$ orbitals. An alternative interpretation is that the emissive excited state is still the cluster core orbital from which intersystem crossing to nonemissive ligand $\pi^*$ orbitals could quench the emission pathway.

The $\phi_{em}$ and $\tau_{em}$ values of the py and mpy complexes are similar to those of $[Re_6(\mu_3\text{-}S)_8Cl_6]^{4-}$, indicating that the natures of the excited states of these complexes are similar. Although direct evidence for the natures of the LUMOs of these complexes from the cyclic voltammetric measurements was not obtained (vide supra), we believe, by taking these photophysical data into account, that the LUMOs of these complexes are more likely to be localized on the cluster cores.

## Conclusion

Preparation methods for a series of hexanuclear octahedral rhenium(III) clusters have now been established in which the number and geometrical configuration of terminal N-heterocyclic ligands are controlled. Versatile redox characteristics of the complexes have been revealed: (i) the $Re^{III}_6/Re^{III}_5Re^{IV}$ redox process is correlated linearly with the ligand p$K_a$ values, with a slope of 0.019 V/p$K_a$, but is independent of the geometry (cis and trans isomers) of the complexes, (ii) the ligand-centered redox processes observed for the pz, bpy, and cpy complexes indicate that the ligand $\pi^*$ orbitals consist the LUMOs of the complexes, (iii) the ligand redox waves show splitting, the extent of which depends on the kinds of ligands and the geometrical configurations of the complexes, and (iv) proton-coupled two-electron redox reactions per one ligand ($Hbpy^{2-}$/bpy) in $[Re_6(\mu_3\text{-}S)_8Cl_4(bpy)_2]^{2-}$ were observed in acetonitrile upon addition of the weak proton donor imidazole. Luminescent properties of the $Re_6$ complexes are further demonstrated for those containing py and its derivatives, suggesting promising photophysical and photochemical studies of the $Re_6$ complexes. Different emissive excited states have been suggested for the first time: cluster core excited states for the complexes with py and mpy ligands and ligand $\pi^*$ orbitals for the bpy, pz, and cpy derivatives.

**Acknowledgment.** Financial support from Grant-in-Aid Nos. 09237106 and 10149102 (Priority Areas of Electrochemistry of Ordered Interfaces and Metal-Assembled Complexes, respectively) is gratefully acknowledged.

**Supporting Information Available:** An X-ray crystallographic file in CIF format, for **1a**. This material is available free of charge via the Internet at http://pubs.acs.org.

IC991282A